© 2023. Published by The Company of Biologists Ltd | Development (2023) 150, dev201373. doi:10.1242/dev.201373

TECHNIQUES AND RESOURCES

RESEARCH ARTICLE

An optimized Tet-On system for conditional control of gene expression in sea urchins

Jian Ming Khor and Charles A. Ettensohn*

ABSTRACT

Sea urchins and other echinoderms are important experimental models for studying developmental processes. The lack of approaches for conditional gene perturbation, however, has made it challenging to investigate the late developmental functions of genes that have essential roles during early embryogenesis and genes that have diverse functions in multiple tissues. The doxycycline-controlled Tet-On system is a widely used molecular tool for temporally and spatially regulated transgene expression. Here, we optimized the Tet-On system to conditionally induce gene expression in sea urchin embryos. Using this approach, we explored the roles the MAPK signaling plays in skeletogenesis by expressing genes that perturb the pathway specifically in primary mesenchyme cells during later stages of development. We demonstrated the wide utility of the Tet-On system by applying it to a second sea urchin species and in cell types other than the primary mesenchyme cells. Our work provides a robust and flexible platform for the spatiotemporal regulation of gene expression in sea urchins, which will considerably enhance the utility of this prominent model system.

KEY WORDS: Echinoderm, Ets1, MAPK signaling, Sea urchin skeletogenesis, Targeted cell ablation, Tet-On inducible system

INTRODUCTION

Sea urchin embryos are a prominent model system for investigating developmental processes, owing to their relatively simple organization, optical transparency, and amenability to experimental manipulation. During development, diverse cell types with transient regulatory states are defined by networks of differentially expressed genes, structured as modular gene regulatory networks or GRNs. The core components of GRNs are temporally and spatially restricted transcription factors (TFs), signaling factors, and the downstream terminal differentiation genes controlled by the regulatory genes. Determining how these combinations of genes, operating within a hierarchical network, drive the morphogenesis of specific anatomical features during development will lead to a better understanding of the connection between genotype and phenotype.

To establish the causal links required for the construction of experimental GRN models, functional perturbations of regulatory genes are usually performed, followed by observation of the effects on potential target genes. Although several approaches have been employed to successfully perturb gene function in sea urchin embryos, functional studies generally rely on microinjection of reagents such as morpholino antisense oligonucleotides (MOs) to block translation or splicing (Yaguchi, 2019), mRNAs encoding dominant-negative or constitutively active forms of proteins (Lepage and Gache, 2004), and targeted genome-editing nucleases, such as transcription activator-like effector nucleases (TALENs) (Yamazaki et al., 2021) and CRISPR-Cas9 (Fleming et al., 2021; Lin et al., 2019; Wessel et al., 2020). These conventional approaches, however, face a common constraint: they do not allow for conditional gene perturbation. As microinjection is normally performed on fertilized eggs, the injected reagent will exert its effects ubiquitously and almost immediately, which consequently limits this approach to early developmental stages. Chemical inhibitors provide more flexibility in the timing of their application, but may lack molecular specificity or produce complex indirect effects as they commonly target signaling pathways that regulate diverse cellular functions, such as cell growth, proliferation and differentiation. A modified version of MOs that can cross cell membranes, termed Vivo-MOs, have been reported to silence genes effectively in sea urchin embryos (Heyland et al., 2014; Luo and Su, 2012), but their use has been limited by low solubility and toxicity (Cui et al., 2017). More recently, caged morpholinos have been used for temporally regulated gene knockdowns in sea urchins (Bardhan et al., 2021).

The skeletogenic GRN that drives the formation of the intricate, calcite-based endoskeleton in sea urchin larvae has been intensively investigated (see reviews by McIntyre et al., 2014; Shashikant et al., 2018). The skeleton is produced by primary mesenchyme cells (PMCs), which are descendants of the four large micromeres that form during early development through the actions of asymmetric division and localized maternal factors. At the mesenchyme blastula stage, the PMCs undergo epithelial-mesenchymal transition (EMT) and ingress into the blastocoel. As the embryo undergoes gastrulation a cell-autonomous program that initially deploys the skeletogenic GRN gradually shifts to become signal dependent. Ectoderm-derived cues, such as vascular endothelial growth factor-3 (VEGF3), guide PMC migration and fusion within the blastocoel to form a distinctive ring-like pattern consisting of two clusters of cells (the ventrolateral clusters) (Adomako-Ankomah and Ettensohn, 2013; Duloquin et al., 2007; Knapp et al., 2012; Morgulis et al., 2019; Sun and Ettensohn, 2014). It is within these two cell clusters that spicule formation is initiated. During later stages of development, signals from the adjacent ectodermal cells continue to stimulate the growth, elongation and branching of skeletal rods that extend from the spicule primordia. Treatment with axitinib, a selective VEGF receptor inhibitor, revealed that VEGF signaling is required for PMC migration and patterning during later stages of development (Adomako-Ankomah and Ettensohn, 2013; Morgulis et al., 2019, 2021). Genes with localized expression at the tips of the growing arms are also downregulated in axitinib-treated

Department of Biological Sciences, Carnegie Mellon University, Pittsburgh, PA 15213, USA.

*Author for correspondence (ettensohn@cmu.edu)

J.M.K., 0000-0002-1428-6770; C.A.E., 0000-0002-3625-0955

Handling Editor: Cassandra Extavour
Received 12 October 2022; Accepted 28 November 2022

Development (2023) 150, dev201373. doi:10.1242/dev.201373

embryos (Morgulis et al., 2019; Sun and Ettensohn, 2014; Tarsis et al., 2022).

The mitogen-activated protein kinase (MAPK) signaling pathway has been shown to be required for sea urchin embryonic skeletogenesis (Fernandez-Serra et al., 2004; Röttinger et al., 2004). Phosphorylated extracellular signal-regulated kinase (ERK), a marker for MAPK pathway activity, is found in the micromere lineage prior to PMC ingression. During gastrulation, activated ERK is detected in the PMC ventrolateral clusters and in the adjacent ectoderm, as well as in secondary mesenchyme cells (SMCs) at the tip of the invaginating archenteron. During later stages of larval development, ERK activation is observed in diverse cell types, such as the coelomic pouches and foregut (Fernandez-Serra et al., 2004). Inhibition of mitogen-activated protein kinase (MEK), an upstream activator of ERK, using U0126 blocks PMC ingression and differentiation (Fernandez-Serra et al., 2004; Röttinger et al., 2004). Overexpression of either dominant-negative MEK or dual specificity phosphatase 6 (DUSP6, also known as MAP kinase phosphatase 3 or MKP3), both of which are known to downregulate ERK activity, also results in inhibition of PMC specification (Fernandez-Serra et al., 2004; Röttinger et al., 2004).

In previous studies, activation of the MAPK signaling pathway in the large micromere lineage was shown to be cell-autonomous. In the early embryo, MAPK signaling is regulated by maternal β-catenin (Röttinger et al., 2004). Additionally, U0126 treatment blocks the formation of spicules and downregulates the expression of biomineralization genes in micromere cultures (Fernandez-Serra et al., 2004). Activated ERK is detected in dissociated blastomeres prior to the hatched blastula stage, at roughly the same time as in control embryos (Röttinger et al., 2004). During later stages of development, dissociated blastomeres exhibit lower levels of activated ERK compared with intact embryos, suggesting that other regulatory inputs are necessary for sustained MAPK activation following the shift from cell-autonomous to signal-dependent regulation of development. In the same studies, skeletogenesis was shown to be inhibited in embryos exposed to U0126 after PMC ingression. Embryos treated with U0126 during later stages of embryonic development exhibit downregulation of biomineralization genes at the growing tips of the anterolateral and postoral rods (Sun and Ettensohn, 2014). As studies in mammalian systems have revealed that VEGF induces MAPK signaling to stimulate various cellular functions (Doanes et al., 1999), these findings point to a possible link between VEGF and MAPK signaling during late stages of sea urchin skeletogenesis, although a direct connection has not been established.

Ets1, a key transcription factor in the sea urchin skeletogenic GRN, was identified as a putative target of ERK phosphorylation (Röttinger et al., 2004). RNA-seq studies have shown that many PMC effector genes are positively regulated by Ets1 (Rafiq et al., 2014). Ets1 expression also coincides with activated ERK during PMC and SMC ingression (Fernandez-Serra et al., 2004; Röttinger et al., 2004). Knockdown of Ets1 with Ets1 MO (Rafiq et al., 2012) or suppression of endogenous Ets1 activity through overexpression of a dominant-negative form of Ets1 (Kurokawa et al., 1999; Sharma and Ettensohn, 2010), phenocopies the effects of U0126 treatment. In contrast, overexpression of a constitutively active form of Ets1 (phosphomimetic Ets1) restores PMC specification in embryos treated with U0126, suggesting that MAPK signaling regulates skeletogenesis through Ets1 phosphorylation (Röttinger et al., 2004).

Like many regulatory and signaling genes, ERK and Ets1 are expressed in diverse embryonic territories and across multiple developmental stages (Fernandez-Serra et al., 2004; Röttinger et al., 2004). Hence, the lack of conditional approaches in the sea urchin model system has made it challenging to define precisely the developmental functions of these proteins. In the current study, we modified and optimized a two-plasmid Tet-On system for inducible transgene expression to explore the roles the MAPK signaling pathway plays in PMC specification and skeletogenesis. The tetracycline-responsive Tet-On and Tet-Off gene expression systems are widely used in many eukaryotic models to control transgene activity (see review by Das et al., 2016). The Tet-On system permits activation of transgene expression by treatment with tetracycline or tetracycline derivatives such as doxycycline (Dox), whereas the Tet-Off system permits transgene silencing through continuous Dox administration. The Tet-On system we used in this study consists of two different components: (1) a third-generation *reverse tetracycline-controlled transactivator* (*rtTA* or *tetON3G*) gene downstream of a sea urchin-specific *cis*-regulatory element (CRE) and promoter and (2) the gene of interest downstream of the tetracycline response element (TRE) and the minimal human cytomegalovirus (CMV) promoter. Technical advancements in inducible gene perturbation such as the work we present here will considerably enhance the utility of sea urchins and other echinoderms as models for developmental studies.

RESULTS

A two-plasmid Tet-On system confers conditional control of transgene expression

The ability to regulate the timing of transgene expression in a cell type-specific manner is a powerful tool in developmental studies. To direct transgene expression spatially and temporally, we optimized a two-plasmid Tet-On system consisting of transactivator and responder constructs (see Materials and Methods). We first placed the *reverse tetracycline-controlled transactivator* (*rtTA*) gene under the control of a *Sp-EMI/TM* intronic *cis*-regulatory element (CRE) (characterized by Khor et al., 2019) and the *Sp-endo16* ubiquitous promoter to generate the transactivator construct PMC-CRE: rtTA (Fig. 1A). We then placed the GFP coding sequence immediately downstream of the TRE and the minimal CMV promoter to generate the responder construct TRE: GFP. As a preliminary test of the functionality of the Tet-On system, we co-injected the plasmids and exposed transgenic *Lytechinus variegatus* embryos to 5 µg/ml Dox (Fig. S1A). Transgenic embryos that had reached the early blastula or late gastrula stage and were then exposed to Dox overnight showed strong GFP fluorescence exclusively in the PMCs (Fig. 1B). The distribution of GFP matched that observed when GFP is under direct, constitutive control of the *Sp-EMI/TM* CRE (Khor et al., 2019). As GFP protein can readily diffuse throughout the PMC syncytium, the entire PMC network is labeled in transgenic embryos, despite the mosaic incorporation and expression of transgenes in sea urchins. In the absence of Dox, GFP protein expression was undetectable, indicating that our Tet-On system conferred conditional control of gene expression.

Optimization of Dox treatment

Although tetracycline and its derivatives, such as Dox, are generally well tolerated by eukaryotic systems, we examined whether Dox exposure can adversely affect sea urchin embryonic development (Fig. S2A). We found that embryos exposed to Dox at various concentrations and different stages developed normally (Fig. S2B).

Development (2023) 150, dev201373. doi:10.1242/dev.201373

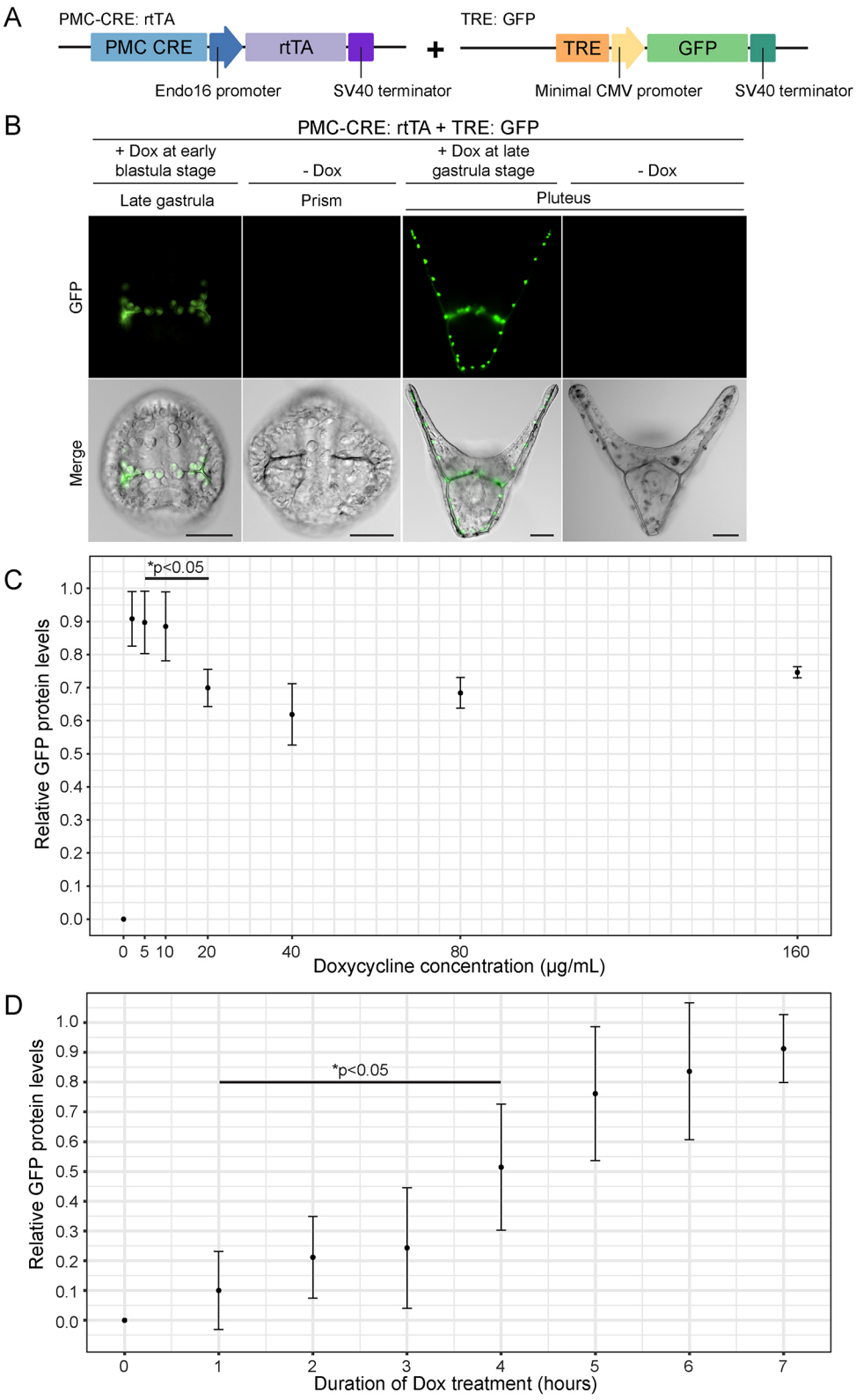

Fig. 1. Inducible gene expression in the sea urchin embryo using the Tet-On system. (A) Schematic of the transactivator and responder constructs used to induce GFP expression in PMCs (see Materials and Methods). (B) GFP expression in the PMCs of transgenic embryos exposed to 5 µg/ml Dox overnight, beginning at the early blastula or late gastrula stage (see Fig. S1A). Top: GFP fluorescence in live embryos. Bottom: GFP fluorescence overlaid onto differential interference contrast (DIC) images. (C) Dose-dependent induction of GFP expression by Dox. Embryos were treated with increasing concentrations of Dox (0, 2, 5, 10, 20, 40, 80 and 160 µg/ml) and relative GFP protein levels were quantified by ELISA (see Fig. S1B). There was a moderate but statistically significant decrease in relative GFP protein levels (1.28-fold) when comparing embryos treated with 5 and 20 µg/ml Dox (see Table S1). (D) Plot showing the time-dependent inducibility of GFP expression following Dox treatment. GFP expression was induced with 5 µg/ml Dox at the late gastrula stage and relative GFP protein levels were quantified by ELISA (see Fig. S1C,D). There was a statistically significant increase in relative GFP protein levels (7.6-fold) at 4 h compared with the first hour of Dox exposure (see Table S1). Error bars represent s.d. from three independently repeated experiments. Scale bars: 50 µm.

We next investigated whether Dox treatment can affect the development of transgenic embryos constitutively expressing rtTA (Fig. S3A). Similarly, we found that transgenic embryos expressing PMC-specific rtTA.mCherry developed normally in the presence of Dox, regardless of the concentration or timing of exposure (Fig. S3B). To examine the Dox dose-dependent response of our Tet-On system, we used ELISA to quantify GFP protein levels in transgenic embryos (PMC-CRE: rtTA+TRE: GFP) treated with various Dox concentrations (Fig. S1B). Although the overall levels of responder inducibility varied between biological replicates (Table S1), we found that induction of GFP expression was highly dose dependent, with maximal activation achieved at Dox

Development (2023) 150, dev201373. doi:10.1242/dev.201373

concentrations ranging from 2 to 10 µg/ml (Fig. 1C). Based on these results, we chose to use 5 µg/ml of Dox for all our experiments, unless stated otherwise. We next evaluated the duration of Dox treatment that was needed for detectable gene expression in transgenic embryos co-injected with PMC-CRE: rtTA and TRE: GFP by measuring GFP protein levels in transgenic embryos exposed to 5 µg/ml Dox from 0 to 7 h (Fig. S1C). We found that a statistically significant increase in relative GFP levels ($*P<0.05$) could be detected via ELISA as early as 4 h after the addition of Dox to the seawater (Fig. 1D). We could also detect GFP expression by fluorescence imaging approximately 3-4 h after the addition of Dox (Fig. S1D). Taken together, our findings show that inducible GFP expression in sea urchin PMCs using the Tet-On system is dependent on the dose and duration of Dox exposure.

PMC-specific induction of transgene expression in *L. variegatus* embryos

Dominant-negative Ets1

To leverage the potential of our Tet-On system for studying sea urchin skeletogenesis, we sought to disrupt genes involved in the MAPK signaling pathway, an essential component of the GRN governing skeletogenic cell fate specification (Fig. S4). Ets1, a downstream target of the MAPK signaling pathway, is a pivotal regulatory gene within the skeletogenic GRN and is required for PMC specification and EMT. The function of Ets1 during late skeletogenic processes, however, has not been explored. A dominant-negative form of Ets1 consisting of only the DNA-binding domain (DBD) has been characterized in previous studies (Kurokawa et al., 1999; Sharma and Ettensohn, 2010). We modified this dominant form by fusing the coding sequences of the repressor domain of *Drosophila melanogaster* Engrailed (Dm-En) with the DBD of *L. variegatus* Ets1 (Lv-Ets1-DBD), and tagged the chimeric protein with GFP, thereby creating dnLv-Ets1.GFP. We then cloned the recombinant gene downstream of the TRE and minimal CMV promoter to generate the responder construct TRE: dnLv-Ets1.GFP (Fig. 2A). To confirm the dominant-negative effects of our chimeric protein, we synthesized and injected capped *dnLv-Ets1.GFP* mRNA into fertilized *L. variegatus* eggs. We confirmed that PMCs failed to ingress and skeletogenesis was inhibited in embryos expressing dominant-negative Ets1, as reported in previous studies (Fig. S5A,B). In contrast, embryos injected with mRNA encoding a chimeric protein consisting of Dm-En and GFP (Dm-En.GFP) developed normally (Fig. S5C).

To induce dnLv-Ets1.GFP expression in PMCs, we co-injected the PMC-CRE: rtTA and TRE: dnLv-Ets1.GFP constructs into fertilized eggs. We exposed the transgenic embryos to Dox at different times and imaged them at various developmental stages (Fig. 2B). We opted to carry out overnight Dox treatment for two primary reasons: (1) based on our initial studies, we anticipated that overnight induction would allow ample time for the transgene transcript and protein to accumulate to functional levels, and (2) differences in skeletal growth between expressing and non-expressing embryos became more apparent over time. We observed that dnLv-Ets1.GFP expression was restricted to specific PMC clonal clusters, likely because of the presence of a nuclear localization signal (NLS) within the Lv-Ets1 DBD, coupled with mosaic incorporation of transgenes in sea urchin embryos during early cleavage stages. This finding was not surprising, as other transcription factors also exhibit highly restricted mobility within the PMC syncytium (J.M.K., J. Guerrero-Santoro and C.A.E., unpublished). Expression of dnLv-Ets1.GFP only on one side of the bilaterally symmetrical embryo allowed us to observe the distinct phenotype caused by perturbation of Ets1 function, as PMCs without transgene expression served as internal controls within the same individual embryos. When embryos were exposed to Dox from the early blastula stage and scored at the late gastrula stage, we found that only a small subset of transgenic embryos with asymmetric dnLv-Ets1.GFP expression exhibited unilateral defects in spicule formation (Fig. 2C). This may be due to the low activity of the *Sp-EMI/TM* CRE during early development (i.e. prior to PMC ingression). Remarkably, however, at later stages of development, asymmetric expression of dnLv-Ets1.GFP almost always coincided with the inhibition of spicule formation or skeletal rod growth and elongation specifically on the side of the embryo where the dominant-negative protein was expressed. Expression of dnLv-Ets1.GFP in PMCs did not appear to affect skeletal structures that had formed prior to induction of the transgene, such as the ventral transverse rods. Exposure to Dox prior to PMC ingression resulted in a pronounced inhibition of spicule formation (Fig. 2Ca, Cb). We also observed PMCs expressing dnLv-Ets1.GFP that did not appear to be associated with the syncytium, and found that such cells were noticeably more prevalent when the transgene was induced in the early embryo prior to PMC fusion (i.e. at the early blastula and mesenchyme blastula stages) than when Dox was added later in development. As many genes involved in PMC migration and fusion are regulated in a positive manner by Ets1 (Ettensohn and Dey, 2017; Khor and Ettensohn, 2022; Saunders and McClay, 2014), we speculate that early induction of dnLv-Ets1.GFP disrupts those cellular processes and prevents transgenic cells from fusing with the PMC syncytium during early development. In contrast, embryos exposed to Dox during the late gastrula stage after PMCs have migrated and fused exhibited shortened body and postoral rods (Fig. 2Cc). When exposed to Dox at the prism stage, growth and elongation of the postoral and anterolateral rods were disrupted in 4-armed plutei (Fig. 2Cd). These findings indicate that Ets1 is not only required for specifying PMCs early in development but also for actively maintaining proper growth and elongation of the skeletal rods.

To characterize the effects of dnLv-Ets1.GFP on the expression of terminal differentiation genes in the PMCs, we used combined whole-mount fluorescent *in situ* hybridization and immunofluorescence staining (ImmunoFISH) to visualize dnLv-Ets1.GFP protein and RNA transcripts of biomineralization genes simultaneously (see Materials and Methods). Both *p16* and *sm30b* are downstream targets of Ets1, based on early knockdown of Ets1 expression and analysis of gene expression at the mesenchyme blastula stage (Rafiq et al., 2014). In control embryos, *p16* was highly expressed at the tips of the actively growing arm rods (the postoral and anterolateral rods) and at the tips of the body rods, in the scheitel region (Fig. 3A,B). In contrast, the *sm30b* gene was highly expressed throughout the PMC syncytium, except for PMCs associated with the ventral transverse rods (Fig. 3A,C). ImmunoFISH staining of transgenic embryos (PMC-CRE: rtTA+TRE: dnLv-Ets1.GFP) revealed that localized dnLv-Ets1.GFP expression in PMCs inhibited *p16* expression at the tip of the nearest arm (Fig. 3D). Expression of dnLv-Ets1.GFP in the ventral transverse rods, however, did not appear to affect *p16* expression in the nearest arm of the 2-armed pluteus. Symmetric expression of dnLv-Ets1.GFP in the ventrolateral clusters of prism-stage embryos also completely abolished *sm30b* expression (Fig. 3E). Asymmetric, localized expression of dnLv-Ets1.GFP in transgenic embryos, however, abolished *sm30b* expression in PMCs only on that side of the bilaterally symmetrical, 2-armed pluteus. The disruption to *sm30b* expression occurred not only in PMCs with detectable levels of dnLv-Ets1.GFP expression, but also in PMCs nearby. These results show for

Development (2023) 150, dev201373. doi:10.1242/dev.201373

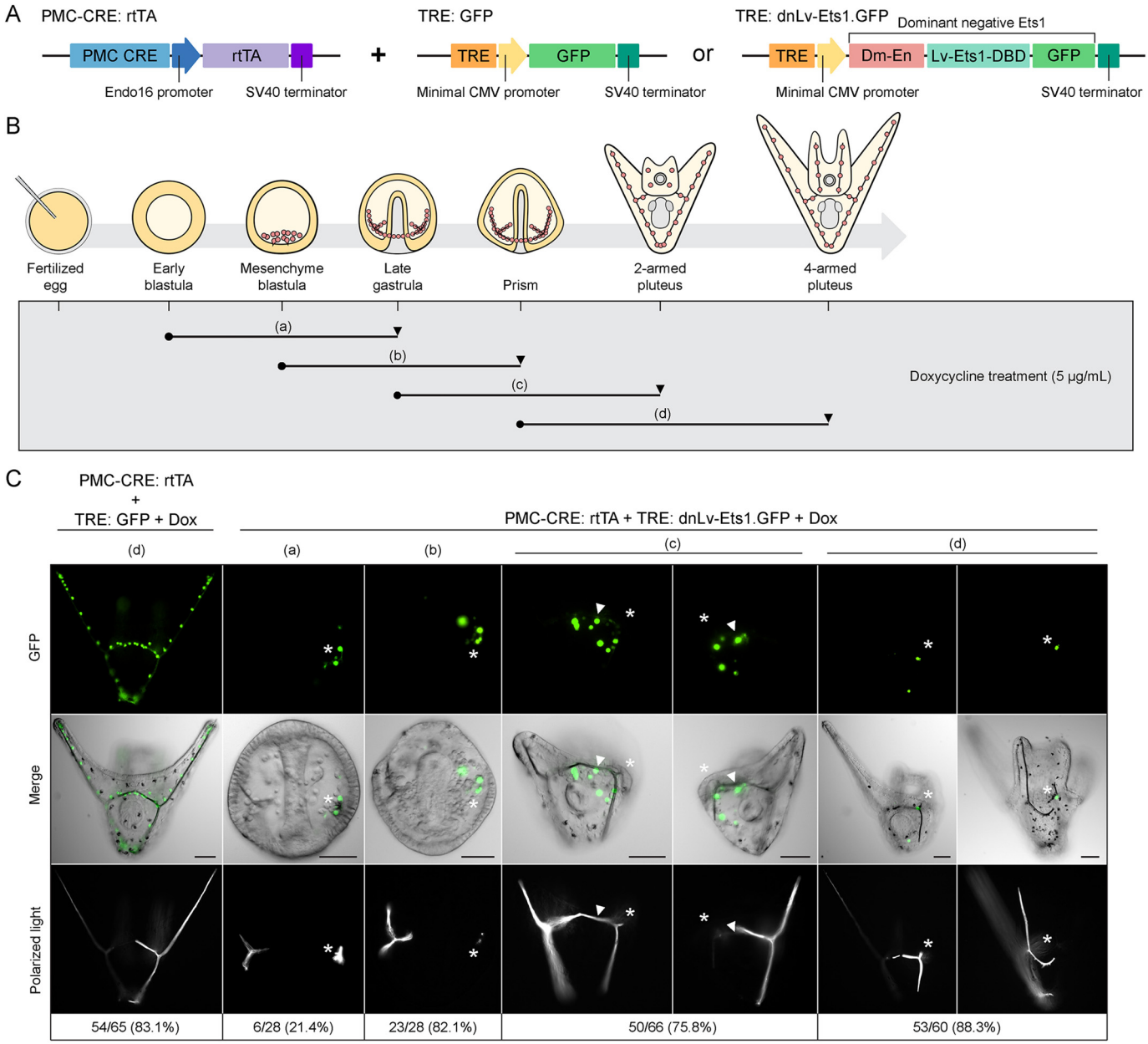

Fig. 2. Localized expression of dominant-negative Ets1 (dnLv-Ets1.GFP) in PMCs disrupts skeletogenesis in transgenic sea urchin embryos. (A) Schematic of the transactivator and responder constructs used to induce PMC-specific GFP or dnLv-Ets1-GFP expression. (B) Experimental design showing the treatment schedules (a-d). Solid circles indicate the stages at which Dox was added. Black arrowheads indicate the stages at which embryos were collected for analysis after overnight Dox treatment. (C) Representative images of transgenic embryos with induced expression of PMC-specific GFP or dnLv-Ets1-GFP (treatment schedules a-d). GFP expression in the PMCs did not affect embryonic skeletogenesis. Induced asymmetric expression of dnLv-Ets1-GFP in PMCs inhibited spicule formation and elongation of skeletal rods (asterisks). The percentage of transgenic embryos showing similar patterns of GFP or dnLv-Ets1-GFP expression and phenotype is shown. White arrowheads indicate ventral transverse rods that developed normally. Top: GFP fluorescence in live embryos. Middle: GFP fluorescence overlaid onto DIC images. Bottom: polarized light images showing skeletal elements. Scale bars: 50 µm.

the first time that positive inputs from Ets1 are required to maintain the expression of PMC terminal differentiation genes during the later stages of sea urchin embryonic development.

Additionally, we also performed immunofluorescence (IF) staining with 6a9, a monoclonal antibody that reacts specifically with the sea urchin MSP130 family of cell-surface proteins, and anti-GFP antibody (Fig. S6A). We found that although localized dnLv-Ets1.GFP expression disrupted the growth and elongation of skeletal elements (except for the ventral transverse rods), GFP-positive PMCs were still strongly labeled with 6a9. *Msp130* is regulated by positively Ets1 (Rafiq et al., 2014) and our data show that two other Ets1-regulated genes (*p16* and *sm30*) exhibited reduced mRNA levels in response to dominant-negative Ets1. Although we did not assess *msp130* mRNA levels directly, we speculate that the persistence in 6a9 immunoreactivity is attributable to the stability of the MSP130 protein (Fig. S6B).

MEK and DUSP6

Next, we sought to utilize the Tet-On system to induce expression of other genes within the MAPK signaling pathway, which has been

Development (2023) 150, dev201373. doi:10.1242/dev.201373

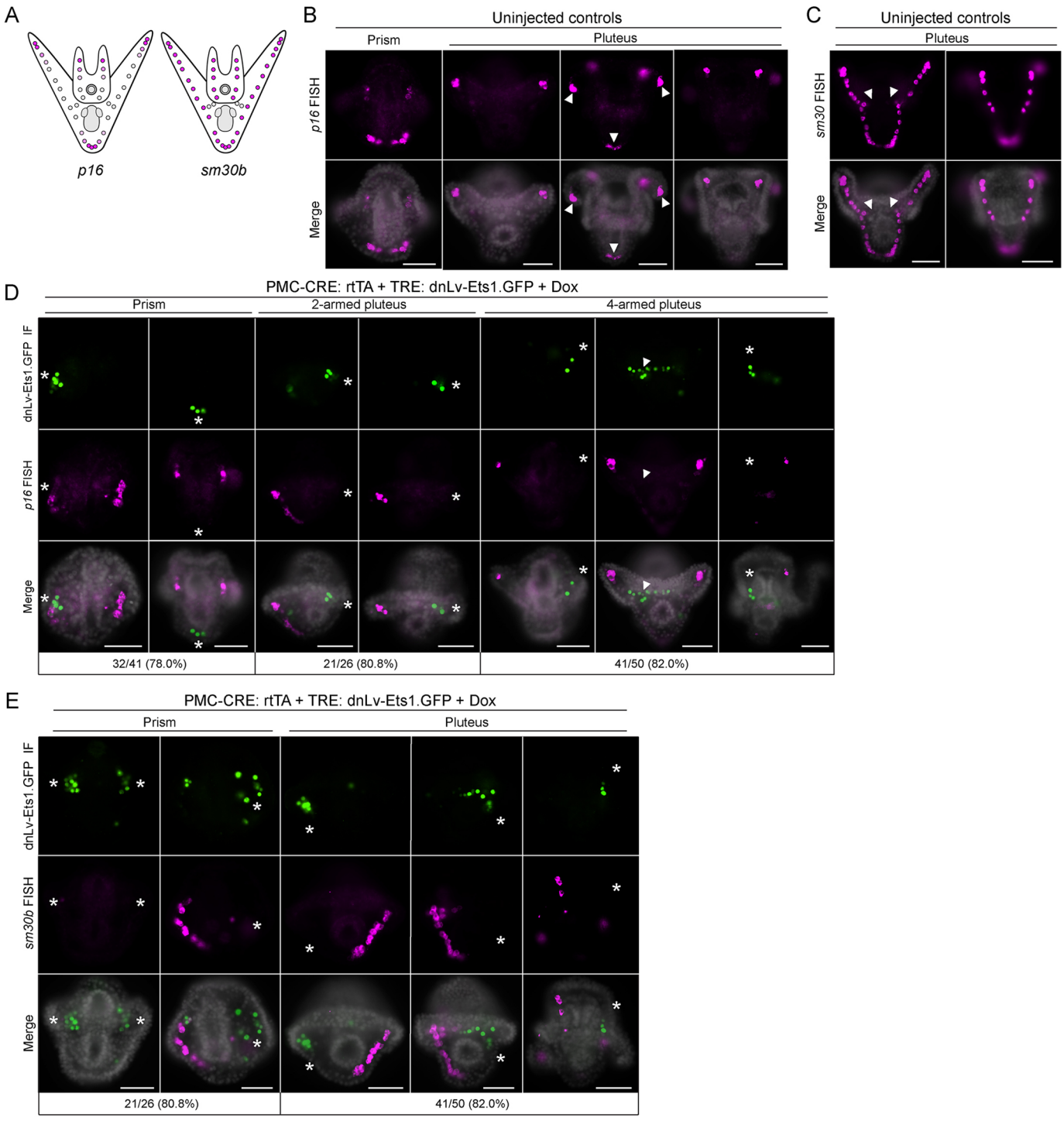

Fig. 3. Localized expression of dominant-negative Lv-Ets1 (dnLv-Ets1.GFP) in PMCs disrupts expression of downstream terminal differentiation genes, *p16* and *sm30b*. (A) Schematic of the expression patterns of *p16* and *sm30b* genes. (B) Single-color FISH images showing strong *p16* expression at the tips of the growing arms and the tips of the body rods (arrowheads) (see Fig. 2B for treatment schedule). (C) Single-color FISH images showing strong *sm30b* expression throughout the PMC syncytial network but not in the ventral transverse rods (arrowheads). (D) GFP and *p16* immunoFISH staining of transgenic embryos with asymmetric dnLv-Ets1.GFP expression in PMCs. The number of embryos expressing dnLv-Ets1.GFP that exhibited reduced *p16* expression in the same region (asterisks) was scored. Expression of dnLv-Ets1.GFP in the ventral transverse rods did not affect *p16* expression in the growing arms of the 4-armed pluteus (arrowheads). Top: GFP-immunostained cells. Middle: Cy3-labeled *p16* RNA transcripts. Bottom: fluorescence merged with Hoechst 33342 counterstain in grayscale. (E) GFP and *sm30b* immunoFISH staining of transgenic embryos with asymmetric dnLv-Ets1-GFP expression in PMCs. The number of embryos expressing dnLv-Ets1.GFP that exhibited reduced *sm30b* expression in the same region was scored. Expression of *sm30b* is also disrupted in PMCs nearby (asterisks). Top: GFP-immunostained cells. Middle: Cy3-labeled *sm30b* RNA transcripts. Bottom: fluorescence merged with Hoechst 33342 counterstain in grayscale. Scale bars: 50 µm.

Development (2023) 150, dev201373. doi:10.1242/dev.201373

shown to regulate Ets1 activity at early developmental stages (Röttinger et al., 2004). We chose to focus on MEK and DUSP6, which are enzymes that regulate ERK (Guo et al., 2020; Muhammad et al., 2018). MEK directly phosphorylates ERK to activate the MAPK signaling pathway, whereas DUSP6 directly dephosphorylates ERK to negatively regulate signaling. The amino acid sequences of the sea urchin MEK and DUSP6 proteins share a high degree of conservation with their human orthologs (Fig. S7). Unlike dnLv-Ets1.GFP, Sp-caMEK.GFP and Sp-DUSP6.GFP do not strictly localize to the nucleus (Figs 4 and 5), demonstrating that these proteins translocate and suggesting that they exert their functions throughout the PMC syncytial network.

To investigate the effects of MEK overexpression in sea urchin embryos, we cloned a constitutively active form of *Strongylocentrotus purpuratus* MEK (S239D/S243D) into the responder construct to generate TRE: Sp-caMEK.GFP (Fig. 4A). The phosphomimetic mutations that we introduced in Sp-caMEK are located in a highly conserved domain that is also found in human MEK1 (Fig. S7A). We first injected capped mRNA containing the coding sequence of Sp-caMEK.GFP into fertilized *L. variegatus* eggs. We found that overexpression of Sp-caMEK.GFP resulted in the formation of ectopic skeletal spicules as well as abnormal branching of skeletal rods (Fig. S8A,B). To induce Sp-caMEK.GFP expression, we co-injected the PMC-CRE: rtTA and TRE: Sp-caMEK.GFP constructs into fertilized eggs. Upon overnight exposure to Dox, the Sp-caMEK.GFP protein was found to be present in all PMCs. We found that late gastrula-stage embryos with Sp-caMEK.GFP expression exhibited ectopic spicule formation (Fig. 4B). In prism and pluteus embryos that were treated with Dox overnight, Sp-caMEK.GFP expression resulted in abnormal branching of the skeletal rods. Using immunoFISH, we also found that Sp-caMEK.GFP overexpression expanded the spatial expression domain of the *p16* gene beyond PMCs that were located near the tips of the growing arms and body rods (Fig. 4C).

We next injected capped mRNA containing the coding sequence of Sp-DUSP6.GFP into fertilized *L. variegatus* eggs. As previously reported by Röttinger et al. (2004), we found that injection of Sp-DUSP6.GFP mRNA into fertilized eggs completely inhibited PMC specification and spicule formation (Fig. S8C,D). We then cloned Sp-DUSP6 into the responder construct to generate TRE: Sp-DUSP6.GFP (Fig. 5A). In prism-stage transgenic embryos that were treated with Dox overnight, Sp-DUSP6.GFP overexpression inhibited spiculogenesis (Fig. 5B). In pluteus-stage embryos that were treated with Dox overnight, Sp-DUSP6.GFP overexpression completely abolished the growth and elongation of the skeletal rods. The Sp-DUSP6.GFP protein was also observed to have translocated throughout the PMC syncytium. ImmunoFISH of transgenic embryos with induced Sp-DUSP6.GFP expression revealed that *p16* expression was completely abolished (Fig. 5C), whereas *sm30b* expression was partially lost in a subset of PMCs (Fig. 5D). Taken together, our findings provide additional evidence that MAPK signaling is essential for the non-uniform patterns of expression within the PMC syncytium following the shift in cell-autonomous to signal-dependent regulation of the skeletogenic GRN. Our observations are consistent with previous studies showing that exposure of whole embryos to a MEK inhibitor (U0126) at later stages inhibited skeletogenesis (Fernandez-Serra et al., 2004; Röttinger et al., 2004). Additionally, these data further support the usefulness of the Tet system for probing the functions of pathways at late developmental stages in situations where inhibitors are not available, with the added advantage of cellular specificity.

Cell type-specific induction of transgene expression in *S. purpuratus* embryos

As many validated CREs have been discovered and tested in *S. purpuratus*, we investigated whether we could use our two-plasmid Tet-On system to drive GFP expression in this species. In the same studies, we also sought to confirm that the Tet-On system could be used to drive gene expression in cell types other than PMCs. In initial experiments, we co-injected the PMC-CRE: rtTA and TRE: GFP constructs into fertilized *S. purpuratus* eggs. Surprisingly, transgenic embryos exposed to Dox at the late gastrula stage showed no observable GFP expression at the early pluteus stage. As the PMC CRE we used was originally derived from *S. purpuratus* and has been shown to drive robust, PMC-specific gene expression in both *S. purpuratus* and *L. variegatus*, this finding pointed to a potential species-specific limitation of the particular pair of transactivator and responder plasmids. To overcome this hurdle, we tested a different combination of transactivator and responder constructs (see Materials and Methods) (Fig. 6A). Transgenic embryos co-injected with the PMC CRE: tetON3G and TRE3Gp: GFP constructs showed strong PMC-specific GFP expression upon overnight exposure to Dox (Fig. 6B). We also co-injected the same pair of constructs into *L. variegatus* embryos and found that they were similarly functional (Fig. 6C).

To take further advantage of the plethora of validated *S. purpuratus* CREs available, we generated tetON3G transactivator constructs containing CREs that can drive cell type-specific expression in the pigment cells (*Sp-pks1* and *Sp-fmo2*) (Khor et al., 2021), gut (*Sp-endo16*) (Yuh and Davidson, 1996) and oral ectoderm (*Sp-nodal*) (Nam et al., 2007). We found that we were able to induce cell type-specific GFP expression upon overnight exposure to Dox (Fig. 6D). Taken together, these results emphasize the wide utility of our Tet-On system as a tool for inducible, cell type-specific gene expression in sea urchins.

Tet-On system for nitroreductase-mediated cell ablation

Targeted cell ablation is a powerful approach for investigating the *in vivo* function of cells. Previous studies have analyzed cell-cell interactions in living sea urchin embryos using fluorescence photoablation (Ettensohn, 1990). Here, we developed a dual input Tet-On system for nitroreductase-mediated cell ablation in sea urchin embryos. Bacterial nitroreductase sensitizes cells to metronidazole (MTZ) by converting the prodrug into a cytotoxic product (Lindmark and Müller, 1976). We cloned a rationally engineered nitroreductase ortholog (NTR 2.0) from *Vibrio vulnificus* (Sharrock et al., 2022) into the Tet-On responder construct to generate TRE: NTR-2.0.GFP (Fig. 7A). We then co-injected the PMC-CRE: rtTA and TRE: NTR-2.0.GFP constructs into fertilized *L. variegatus* eggs. Transgenic embryos were first exposed to Dox at the early blastula stage (Fig. 7B). At the late gastrula stage, a subset of the transgenic embryos was treated with MTZ overnight. We found that overexpression of NTR 2.0 without MTZ exposure did not affect embryonic development (Fig. 7C). In contrast, exposing transgenic embryos with NTR-2.0.GFP expression to MTZ resulted in PMC cell death as well as disruption to the growth and elongation of the pluteus arms and skeletal rods. We also observed that MTZ treatment did not affect transgenic sea urchin embryo development without NTR-2.0.GFP expression. IF staining of a PMC cell surface marker (MSP130) and GFP revealed that the expression of NTR-2.0.GFP, in combination with MTZ treatment, resulted in PMC ablation and disordered PMC syncytial cables (Fig. 7D). The dual-input requirement of this system allows for improved control of targeted cell ablation in two steps: (1) Dox induction permits NTR-2.0 GFP to accumulate within cells, and

Development (2023) 150, dev201373. doi:10.1242/dev.201373

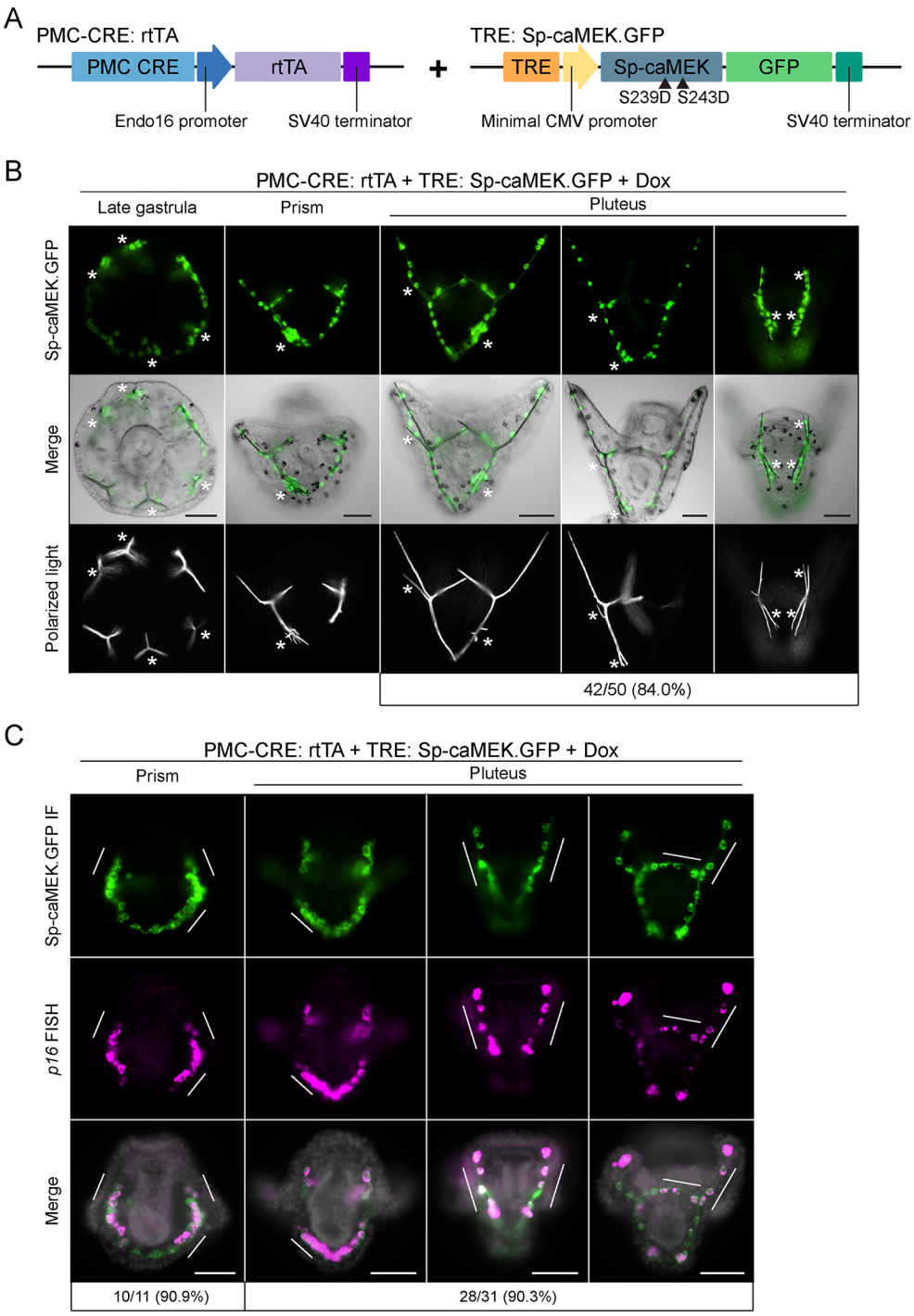

Fig. 4. Induced expression of constitutively active *S. purpuratus* MEK (Sp-caMEK.GFP) in PMCs disrupts skeletal patterning. (A) Schematic of the transactivator and responder constructs used to induce Sp-caMEK.GFP expression in PMCs. (B) Representative images of transgenic embryos expressing Sp-caMEK.GFP after overnight Dox treatment (see Fig. 2B for treatment schedule). The protein is distributed throughout the PMC syncytial network, resulting in supernumerary spicules and abnormal skeletal branching (asterisks). The number of embryos with Sp-caMEK.GFP expression that showed the abnormal skeletal branching phenotype is indicated. Top: GFP fluorescence in live embryos. Middle: GFP fluorescence overlaid onto DIC images. Bottom: polarized light images showing skeletal elements. (C) GFP and *p16* immunoFISH staining of transgenic embryos expressing Sp-caMEK.GFP showed expansion of the *p16* expression domain (white bars). The number of embryos expressing Sp-caMEK.GFP that showed expanded *p16* expression was scored. Top: GFP-immunostained cells. Middle: Cy3-labeled *p16* RNA transcripts. Bottom: fluorescence merged with Hoechst 33342 counterstain in grayscale. Scale bars: 50 µm.

(2) subsequent addition of MTZ causes rapid ablation as cells are already primed with the enzyme.

DISCUSSION

Sea urchins and other echinoderms are powerful models for studying developmental processes and the GRNs that govern them. There are diverse tools available for manipulating gene expression in echinoderm embryos. Most functional studies involve the microinjection of MOs, which often leads to specific and efficient gene knockdowns. Recent studies have also used CRISPR/Cas9 gene editing to explore gene function (Fleming et al., 2021; Lin et al., 2019; Wessel et al., 2020). Another widely used approach is the microinjection of mRNAs, typically encoding dominant-negative or constitutively active proteins. As MOs, CRISPR reagents and mRNAs are usually microinjected into fertilized eggs, a major limitation of these perturbations is that they are uncontrolled spatially and temporally, i.e. they affect most or all cells of the embryo from the onset of development until the reagent (MO or mRNA) declines in abundance to non-functional levels. Chemical inhibitors can partly overcome this hurdle by allowing control over the timing of their application. Not all molecules of pathways can be targeted by inhibitors, however, and inhibitors can produce unintended side effects, owing to a lack of specificity or the pleiotropic nature of their targets.

Development (2023) 150, dev201373. doi:10.1242/dev.201373

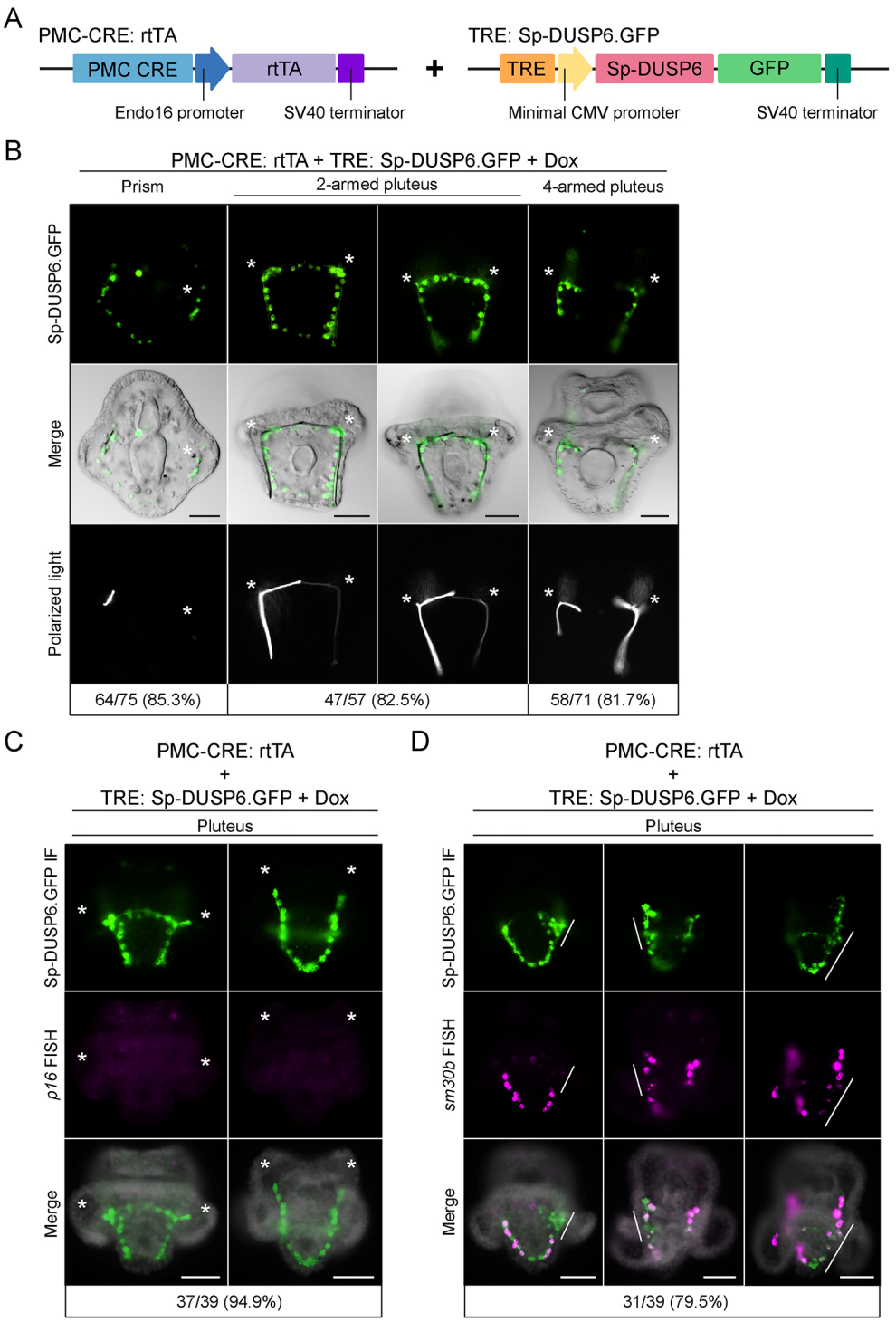

Fig. 5. Induced expression of *S. purpuratus* DUSP6 (Sp-DUSP6.GFP) in PMCs inhibits skeletogenesis. (A) Schematic of the transactivator and responder constructs used to induce Sp-DUSP6.GFP expression in PMCs. (B) Representative images of transgenic embryos expressing Sp-DUSP6.GFP after overnight Dox treatment (see Fig. 2B for treatment schedule). The protein is distributed throughout the PMC syncytial network, inhibiting spicule formation and skeletal growth (asterisks). The number of embryos with Sp-DUSP.GFP expression that showed an abnormal skeletal growth and elongation phenotype was scored. Top: GFP fluorescence in live embryos. Middle: GFP fluorescence overlaid onto DIC images. Bottom: polarized light images showing skeletal elements. (C) GFP and *p16* immunoFISH staining of transgenic embryos expressing Sp-DUSP6-GFP in PMCs showing loss of *p16* expression (asterisks). The number of embryos expressing Sp-DUSP6.GFP that exhibited reduced *p16* expression was scored. Top: GFP-immunostained cells. Middle: Cy3-labeled *p16* RNA transcripts. Bottom: fluorescence merged with Hoechst 33342 counterstain in grayscale. (D) GFP and *sm30b* immunoFISH staining of transgenic embryos expressing Sp-DUSP6.GFP showing partial loss of *sm30b* expression in some PMCs (white bars). The number of embryos expressing Sp-DUSP6.GFP that exhibited reduced *sm30b* expression was scored. Top: GFP-immunostained cells. Middle: Cy3-labeled *sm30b* RNA transcripts. Bottom: fluorescence merged with Hoechst 33342 counterstain in grayscale. Scale bars: 50 µm.

As many sea urchin genes show dynamic changes in their spatiotemporal expression patterns during development, the inability to perturb them conditionally in a cell type-specific manner is a major obstacle in investigating the late developmental functions of genes, especially those that have crucial roles during early embryogenesis. With respect to GRN biology, the lack of targeted approaches has made it difficult to analyze dynamic changes in network circuitry, for example to determine whether a regulatory gene with an important early function continues to provide regulatory inputs at later developmental stages or, alternatively, hands off its regulatory function to downstream transcription factors. In addition, as most regulatory genes are expressed in multiple territories, embryo-wide perturbations can lead to significant inaccuracies in the construction of cell type-specific GRN models. The ability to regulate gene perturbations in sea urchins would make it possible for the direct interrogation of GRN circuitry at late developmental stages and/or in specific tissues.

In the present study, we developed and optimized a two-plasmid Tet-On system for inducible gene expression in sea urchin embryos. In line with our goal of controlling the time of activation of our genes of interest, we opted to use the Tet-On system rather than Tet-

Development (2023) 150, dev201373. doi:10.1242/dev.201373

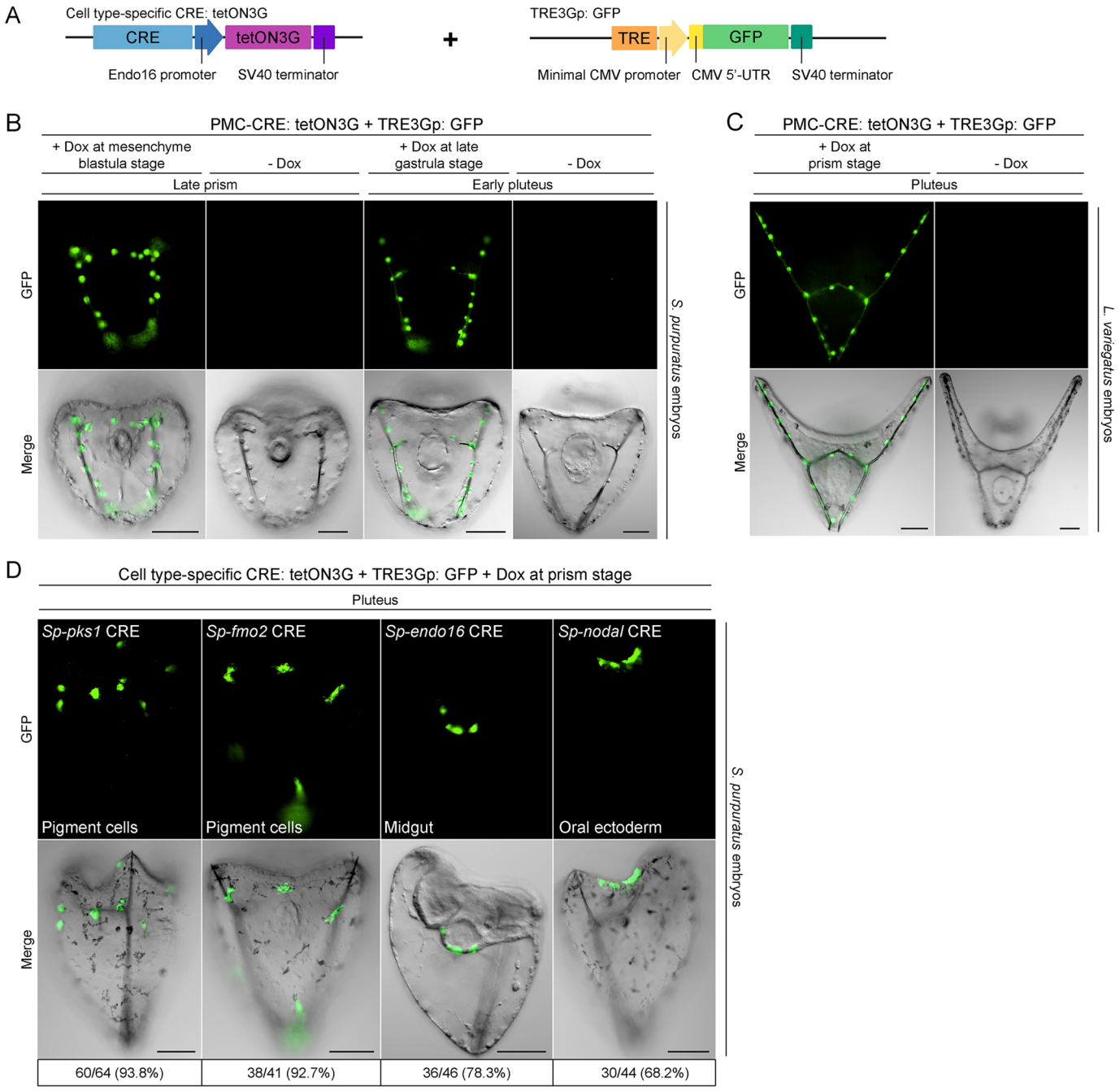

Fig. 6. Inducible gene expression in diverse cell types using the Tet-On system. (A) Schematic of the transgenic activator and responder constructs used to induce GFP expression in *S. purpuratus* embryos (see Materials and Methods). (B,C) GFP expression in the PMCs of transgenic *S. purpuratus* (B) and *L. variegatus* (C) embryos exposed to 5 µg/ml Dox overnight at the late gastrula stage. GFP fluorescence was not observed when embryos were not exposed to Dox. Top: GFP fluorescence in live embryos. Bottom: GFP fluorescence overlaid onto DIC images. (D) GFP expression in different cell types of transgenic embryos exposed to 5 µg/ml Dox overnight at the late gastrula stage. The number of embryos with GFP fluorescence showing expression in the expected cell types was scored. Top: GFP fluorescence in live embryos. Bottom: GFP fluorescence overlaid onto DIC images. Scale bars: 50 µm.

Off, as the latter would require long-term exposure to Dox to prevent constitutive expression. As a proof of concept, we demonstrated the feasibility of the system by inducing the expression of GFP exclusively in the PMCs. Our ELISA time course and *in vivo* fluorescence microscopy show that GFP expression driven by PMC-CRE: rtTA can be detected at least as early as 4 h after the addition of Dox. Because it takes some time for transcription, translation and GFP folding, it seems conservative to conclude that, in this case, GFP transcription begins no later than ∼3 h after the addition of Dox. It is important to note, however, that the rate and extent of transgene expression will be construct and protein specific, as different CREs drive different levels of rtTA expression, and because the kinetics of transgene expression at the protein level depend on several additional factors, including the stability of the various mRNA and protein products. The kinetics of gene expression are relatively slow compared with the very rapid development of sea urchins, and this should be taken into consideration when designing experiments. In addition, although

Development (2023) 150, dev201373. doi:10.1242/dev.201373

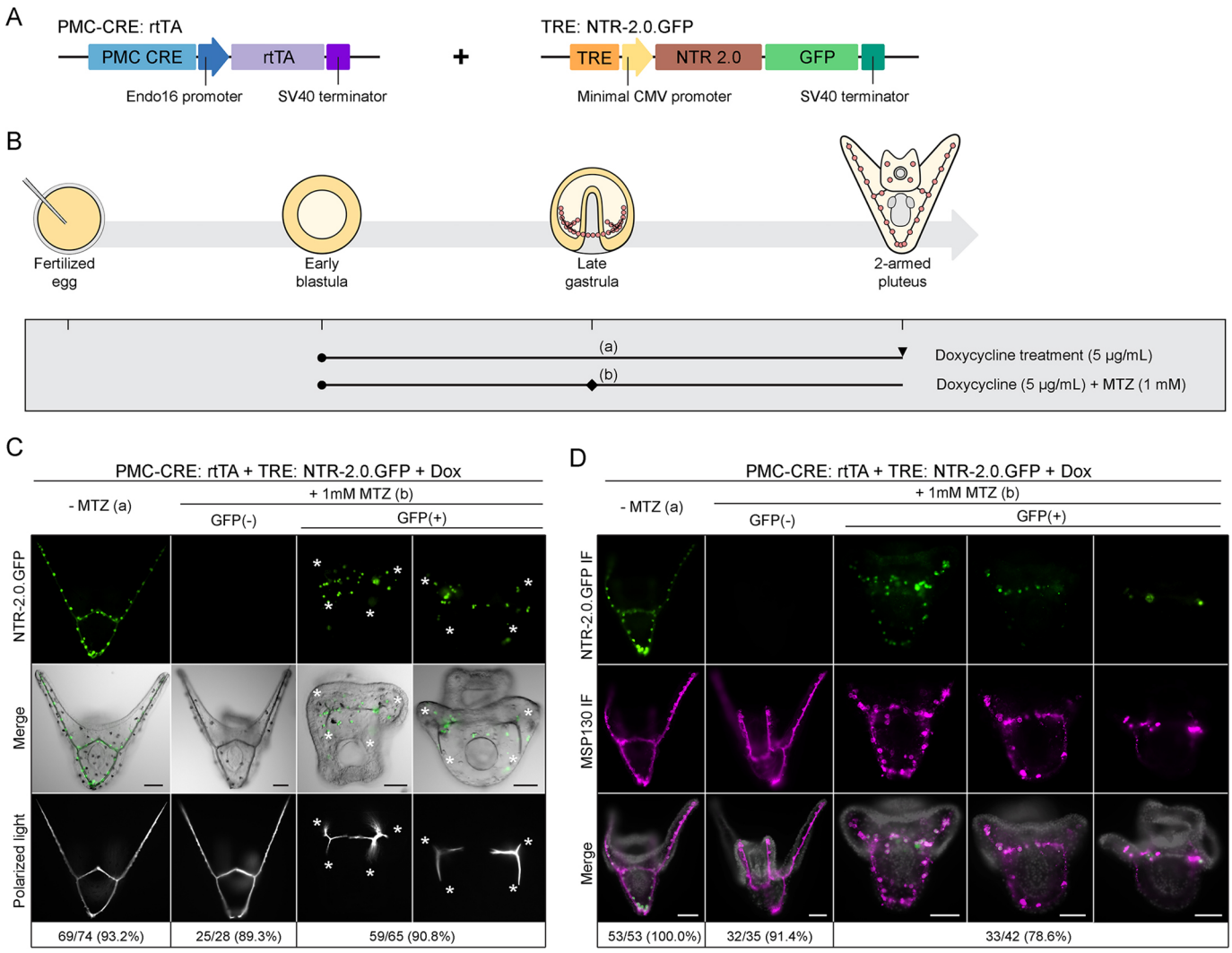

Fig. 7. Dual-input Tet-On system for nitroreductase-mediated cell ablation in sea urchin embryos. (A) Schematic of the transactivator and responder constructs used to induce nitroreductase (NTR-2.0.GFP) expression in PMCs. (B) Experimental design showing the treatment schedule (a,b). Solid circles indicate the stage at which Dox was added. Diamond represents the stage at which metronidazole (MTZ) was added. Arrowhead indicates the stage at which embryos were collected for analysis after overnight Dox treatment. (C) Induced expression of NTR-2.0.GFP and the addition of MTZ resulted in targeted ablation of PMCs and inhibition of skeletogenesis (asterisks). Top: GFP fluorescence in live embryos. Middle: GFP fluorescence overlaid onto DIC images. Bottom: polarized light images showing skeletal elements. The number of embryos with phenotypes similar to the representative images was scored. (D) PMC marker (MSP130) and GFP IF staining of transgenic embryos expressing NTR-2.0.GFP in PMCs. Expression of NTR-2.0.GFP and in combination with MTZ treatment disrupted the PMC syncytial cables. The number of embryos with phenotypes similar to the representative images was scored. Top: GFP-immunostained cells. Middle: MSP130-immunostained skeletal structures (6a9 antibody). Bottom: fluorescence merged with Hoechst 33342 counterstain in grayscale. Scale bars: 50 µm.

the Tet-On system is very useful for the spatiotemporal control of transgene activation and expression, it is less well suited for driving gene expression transiently, i.e. in an 'off-on-off' manner. It has been shown in other model organisms that transgene expression levels gradually decrease after Dox withdrawal, but over a relatively long time frame. For example, in mammalian cell lines, the time required to detect a significant loss of expression can vary from 4 to 14 days depending on cell type (Akhtar and Breunig, 2017). In practice, the speed of reversibility is affected by several factors: the high affinity of Dox for rtTA, the level of rtTA expression (which in our system is partly determined by the properties of the CRE driving rtTA expression), and the perdurance of the mRNA and protein products of the Dox-responsive transgene. Recently, efforts have been taken to produce more rapid loss of transgene expression following Dox withdrawal by fusing protein destabilization sequences to expressed proteins (Pedone et al., 2019), but this strategy has the danger of reducing protein expression to non-functional levels.

Our protein-based assays (quantitative ELISA and *in vivo* fluorescence) indicate that if there is any Dox-independent expression of GFP, it is very low compared with the very robust expression we observe following the addition of Dox. We cannot, however, rule out the possibility of low levels of leaky expression that might be important in some contexts, for example when studying a gene expressed at low levels, or for long-lived transcripts or proteins, which might accumulate prior to induction. The leakiness of transgene expression will depend on the CRE used and the cell type carrying the transgene. Therefore, in practice, if low levels of Dox-independent expression are a significant concern, it will be important for investigators to assess

Development (2023) 150, dev201373. doi:10.1242/dev.201373

the extent of such expression using the specific constructs and cell types of interest.

We have demonstrated the utility of the Tet-On system by using it to induce the expression of genes involved in the MAPK signaling pathway, a pivotal regulator of the sea urchin skeletogenic GRN. Two major components of the pathway, ERK and Ets1, are expressed in several cellular territories across a broad range of developmental stages (Fernandez-Serra et al., 2004; Röttinger et al., 2004). Hence, they are of special interest as candidates for possessing late developmental roles. Ets1 is a key transcription factor required for early PMC specification, and the Ets1 DBD has been shown to exert a dominant-negative function when overexpressed (Kurokawa et al., 1999; Sharma and Ettensohn, 2010). Although the mechanism behind this effect is not entirely clear, we postulate that overexpression of the Ets1 DBD that lacks the transactivation domain outcompetes endogenous Ets1 for DNA-binding sites. In this study, we fused the *L. variegatus* Ets1 DBD to the repressor domain of *Drosophila* Engrailed (Margolin et al., 1994), which efficiently converted the chimeric protein into an obligate repressor (dnLv-Ets1.GFP). We determined the pivotal role of Ets1 in regulating late stage skeletogenesis by inducing dnLv-Ets1.GFP expression at different developmental stages. Mosaic transgenesis in the present study offered a unique advantage when expressing a nuclear protein such as dnLv-Ets1.GFP, which exhibits limited mobility within the PMC syncytium. For instance, it was possible to observe the distinct phenotype caused by disruption of Ets1 function on one side of the bilaterally symmetrical embryo, with PMCs without transgene expression serving as internal controls within the same embryos. We also observed that dnLv-Ets1.GFP locally disrupted the expression of biomineralization genes only in the vicinity of the transgenic cells. Significantly, dnLv-Ets1.GFP expression appeared to only inhibit skeletal elements that were actively growing at the time of induction. We observed that the late function of Ets1 was restricted to the postoral and anterolateral rods in 2-armed and 4-armed plutei, where VEGF3 is highly expressed by the adjacent ectoderm (Adomako-Ankomah and Ettensohn, 2013; Duloquin et al., 2007). In mammalian systems, VEGF stimulates the MAPK signaling pathway, thereby regulating cell proliferation and differentiation (Doanes et al., 1999). Although both inputs are required for sea urchin skeletogenesis, a direct association between VEGF and MAPK signaling has not been established. Our analysis has for the first time directly probed the regulatory circuitry of the PMC GRN at post-blastula stages, when signals from VEGF and the MAPK pathway locally regulate skeletal growth and has shown that Ets1 provides essential, late inputs into biomineralization genes. These findings are consistent with the hypothesis that the VEGF and MAPK pathways act through Ets1, which at early developmental stages is regulated positively by MAPK signaling.

Activated ERK is expressed by many different groups of cells during sea urchin development. Previous studies have reported that MAPK signaling is required for PMC and pigment cell specification, skeletogenesis and gut formation (Fernandez-Serra et al., 2004; Röttinger et al., 2004). Owing to the diverse tissue and developmental processes regulated by MAPK, the common approach of using chemical inhibitors makes it challenging to pinpoint the direct role of MAPK signaling in regulating sea urchin skeletogenesis. Significantly, it has not been possible to determine whether ERK/MAPK signaling acts cell-autonomously within PMCs to regulate skeletogenesis or indirectly through effects on other tissues. Using the Tet-On system to induce expression of constitutively active MEK (Sp-caMEK.GFP) or DUSP6 (Sp-DUSP6.GFP) exclusively in PMCs, we were able to target ERK activity in a cell type-specific manner. We observed that embryos overexpressing Sp-caMEK.GFP exhibited dramatic, ectopic skeletal branching. Ectopic Sp-caMEK.GFP expression resulted in upregulation of *p16* throughout the PMC syncytium and slightly elevated expression of *p16* at the tips of the growing arms, where it is normally expressed (Sun and Ettensohn, 2014). In contrast, ectopic Sp-DUSP6.GFP overexpression phenocopied late-stage U0126 treatment and we observed only a partial loss of *sm30b* expression. These findings raise the possibility that factors other than ERK activity are involved in regulating downstream biomineralization genes such as *p16* and *sm30b*, although an alternative interpretation is that these molecular perturbations only partially disrupted ERK signaling.

It is widely thought that the embryonic skeleton arose within echinoderms via co-option of the adult skeletogenic program, as evidenced by the many similarities in the GRN of skeletogenic cells in the embryo and adult (Czarkwiani et al., 2013; Gao and Davidson, 2008; Gao et al., 2015; Killian et al., 2010). Significantly, the work we describe here allows for higher resolution dissection of the embryonic skeletogenic GRN by decoupling the early, cell-autonomous, and late, signal-dependent modes of skeletogenesis. As the MAPK signaling pathway is activated cell-autonomously in the early embryo, possibly through the actions of localized maternal factors such as β-catenin (Fernandez-Serra et al., 2004; Röttinger et al., 2004), we propose that the heterochronic shift in the deployment of the skeletogenic GRN that occurred during euechinoid evolution was achieved by an important evolutionary innovation that placed MAPK signaling under maternal control. We favor a model whereby current regulatory mechanisms that underlie late embryonic skeletal patterning and growth reflect an ancient heterochronic shift in VEGF3 expression by ectodermal cells (Morino et al., 2012; Yamazaki et al., 2021). We hypothesize that VEGF3 activates Ets1 through the MAPK signaling pathway at late embryonic stages, circuitry that is likely to be similar to the ancestral skeletogenic GRN found in the adult.

To confirm the broader utility of the Tet-On system in sea urchins, we applied it to a second species, *S. purpuratus*. In preliminary experiments, we found that the transactivator and responder constructs used in *L. variegatus* embryos in our initial studies were not functional in *S. purpuratus*. We fully resolved this issue by using a different combination of constructs (tetON3G and TRE3Gp). The rtTA-advanced and tetON3G transactivators are distinct by only three amino acid changes and the TRE3Gp responder contains an additional CMV 5′-UTR downstream of the promoter. We showed that the new combination of transactivator and responder is also highly effective in *L. variegatus* embryos. While testing the different combinations of transactivator and responder plasmids in different sea urchin species, we observed that the common denominator for inducible expression was the presence of the CMV 5′-UTR directly upstream of GFP in the responder construct (data not shown). This region could play a role in regulating transcription from the nearby promoter, the stability of the transcript, or the translational efficiency of the mRNA. It is unclear why this region was required for robust transgene expression in *S. purpuratus* but not *L. variegatus*, although there may be differences in the proteins that interact with this region in the two species. Thus, in the absence of additional information regarding possible species-specificity of the expression system, we recommend that the tetON3G and TRE3Gp constructs be used in future applications. Using validated *S. purpuratus* CREs, we further

Development (2023) 150, dev201373. doi:10.1242/dev.201373

showed that the Tet-On system can be used to induce gene expression in diverse cell types, a demonstration of the capabilities of the system. In the future, the Tet-On system will serve as a flexible platform for the spatiotemporal regulation of gene expression in sea urchins and other echinoderms, thereby enhancing the utility of these model organisms for developmental studies.

MATERIALS AND METHODS

Animals

Adult *Lytechinus variegatus* were acquired from Pelagic Corp (Sugarloaf Key, FL, USA). Adult *S. purpuratus* were obtained from Pete Halmay (San Diego Fishermen's Working Group, CA, USA). Spawning was induced by intracoelomic injection of 0.5 M KCl. *L. variegatus* embryos were cultured in artificial seawater (ASW) at 18-25°C in temperature-controlled incubators whereas *S. purpuratus* embryos were cultured at 15°C. Feeding-stage *L. variegatus* larvae were fed with *Rhodomonas lens* algae.

Plasmid constructs

The EpGFPII plasmid (Cameron et al., 2004), which contains the sea urchin-specific *S. purpuratus endo16* (*Sp-endo16*) basal promoter, was used as a backbone vector. Several changes were introduced to the plasmid; most significantly, the *S. purpuratus cyIIa* leader sequence positioned immediately upstream of the GFP coding sequence was removed and the minimal SV40 terminator sequence was replaced with a longer version of the SV40 poly(A) terminator sequence (see supplementary Materials and Methods for further details).

Transgenic activator constructs

The *rtTA* recombinant gene, based on the *rtTA-Advanced* sequence from pSLIK-Neo (Shin et al., 2006), was synthesized as gBlock gene fragments with and without an mCherry tag by Integrated DNA Technologies. The gBlocks were cloned into EpGFPII in place of the GFP coding sequence downstream of the *Sp-endo16* promoter. To drive PMC-specific expression, an *Sp-EMI/TM* intronic CRE (characterized by Khor et al., 2019) was cloned upstream of the promoter to generate PMC-CRE: rtTA and PMC-CRE: rtTA.mCherry. For inducible GFP expression in *S. purpuratus* embryos, a different transactivator and responder pair was used. The *tetON3G* recombinant gene, based on the transactivator sequence from pCAG-TetON-3G (Faedo et al., 2017), was synthesized as a gBlock gene fragment by Integrated DNA Technologies. CREs that were shown to drive expression specifically in the pigment cells (*Sp-pks1* and *Sp-fmo2*) (Khor et al., 2021), gut (*Sp-endo16*) (Yuh and Davidson, 1996) and oral ectoderm (*Sp-nodal*) (Nam et al., 2007) were cloned upstream of the *tetON3G* gene (see supplementary Materials and Methods for further details).

Transgenic responder constructs

The TRE and minimal CMV promoter were PCR-amplified from pInducer20 (Meerbrey et al., 2011) and cloned upstream of the GFP coding sequence to generate TRE: GFP. The *Drosophila* Engrailed repressor domain (Dm-En) coding sequence was PCR-amplified from genomic DNA (Margolin et al., 1994). The coding sequences for *L. variegatus* Ets1 DBD (Lv-Ets1-DBD), constitutively active/phosphomimetic *S. purpuratus* MEK (LOC576066, Sp-caMEK S239D/S243D) (Brunet et al., 1994), *S. purpuratus* dual specificity phosphatase 6 (LOC115919104, Sp-DUSP6) and *Vibrio vulnificus* nitroreductase (NTR-2.0) (Sharrock et al., 2022) were synthesized as gBlock gene fragments with flanking restriction sites by Integrated DNA Technologies and cloned upstream of GFP in the TRE: GFP construct (see supplementary Materials and Methods for further details). For inducible GFP expression in *S. purpuratus* embryos, the TRE3Gp promoter containing the TRE, minimal CMV promoter and CMV 5′-UTR was cloned upstream of the GFP coding sequence to generate TRE3Gp: GFP (Kang et al., 2019).

Capped mRNA synthesis

Capped mRNAs were synthesized using the mMessage mMachine SP6 Transcription Kit (Invitrogen/Thermo Fisher Scientific). PCR products containing a 5′ SP6 promoter and a 3′ SV40 poly(A) terminator sequence were used as templates for the *in vitro* transcription reactions (see supplementary Materials and Methods for further details).

Microinjection

Linearized plasmids were injected into fertilized *L. variegatus* eggs following established protocols (Arnone et al., 2004; Cheers and Ettensohn, 2004). Each 20 µl injection solution contained 75 ng of the transactivator plasmid, 75 ng of the responder plasmid, 500 ng of HindIII-digested genomic DNA, 0.12 M KCl, 20% glycerol and 0.1% Texas Red-Dextran (10,000 MW). Linear DNA injected into fertilized sea urchin eggs forms a large concatemer that is randomly inherited by one or a few cells during cleavage (McMahon et al., 1985). For mRNA overexpression assays, each 5 µl injection solution contained 1.0 µg/µl mRNA, 0.12 M KCl, 20% glycerol and 0.1% Texas Red-Dextran (10,000 MW).

Embryo culture drug treatments

A 10 mg/ml stock solution of Dox (doxycycline hyclate, D9891, Sigma-Aldrich) was prepared in sterile H_2O and stored in light-protected microcentrifuge tubes at −20°C. Dox was added directly to cultures at different developmental stages for overnight treatment. MTZ (M3761, Sigma-Aldrich) was dissolved directly in ASW to obtain a final concentration of 1 mM. To induce nitroreductase-mediated cell ablation, embryos were collected by centrifugation (1000 ***g*** for 1 min) and resuspended in ASW containing 1 mM MTZ and 5 µg/ml Dox.

GFP ELISA

To determine the effect of Dox concentration on transgene expression, approximately 3000 eggs were injected with PMC-CRE: rtTA and TRE: GFP and incubated at 20°C overnight. The embryos were then pooled at the late gastrula stage and divided into eight parallel cultures. GFP expression was induced overnight using a range of Dox concentrations (0, 2, 5, 10, 20, 40, 80 and 160 µg/ml). At the 2-armed pluteus stage (approximately 48 h post-fertilization), protein was extracted from the eight cultures using the lysis buffer from the GFP Fluorescent ELISA Kit (ab229403) (Abcam) that was supplemented with Halt Protease Inhibitor Cocktail (Thermo Fisher Scientific). The total protein concentration for each culture was measured using the Pierce BCA Protein Assay Kit (Thermo Fisher Scientific). Using the same amount of total protein from each sample, GFP concentration was then determined using the GFP Fluorescent ELISA Kit. Relative GFP levels were then calculated using min-max normalization. To determine the earliest time point at which Dox-induced GFP expression could be detected, approximately 3000 eggs were injected and incubated at 23°C overnight. The embryos were then pooled at the late gastrula stage and divided into eight cultures. GFP expression was induced by the addition of 5 µg/ml Dox. Total protein was then extracted every hour (0, 1, 2, 3, 4, 5, 6 and 7 h post-Dox treatment) and GFP levels were measured using the GFP Fluorescent ELISA Kit as described above. Statistical analysis between different samples was conducted using two-tailed *t*-tests.

ImmunoFISH

ImmunoFISH was employed to visualize *p16* or *sm30b* transcripts and GFP protein simultaneously. DNA templates for RNA probe synthesis were PCR-amplified with reverse primers that contained a T3 promoter sequence (see supplementary Materials and Methods for further details). Digoxigenin-labeled RNA probes were synthesized using the MEGAscript T3 Transcription Kit (Invitrogen/Thermo Fisher Scientific). The single-color fluorescent *in situ* hybridization (FISH) portion of the protocol was carried out as previously described (Ettensohn et al., 2007; Sharma and Ettensohn, 2010) with a few modifications. Embryos were collected and fixed at the desired stage for 1 h in 4% paraformaldehyde in ASW followed by at least 15 min incubation in ice-cold 100% methanol. Fixed embryos were processed immediately or stored in 100% methanol at −20°C. After overnight probe hybridization at 55°C, the samples were washed with PBS containing 0.1% Tween-20 (PBST) and transferred to round-bottom 96-well plates. The samples were then blocked for 1 h at room temperature in PBS containing 4% goat serum, 4% sheep serum and 1%

bovine serum albumin. This was followed by a 2-h incubation in an antibody mixture composed of a 1:1000 dilution of anti-digoxigenin-POD (Roche/Sigma-Aldrich) and a 1:500 dilution of anti-GFP antibody (ab6556) (Abcam) in blocking buffer at room temperature. After several washes with PBST, the samples were incubated in 1:500 DyLight 488 anti-rabbit IgG (Jackson ImmunoResearch Laboratories) for 2 h at room temperature. Following several additional PBST washes, the samples were incubated in a 1:100 dilution of Cy3-Tyramide Signal Amplification Solution (TSA plus Cyanine 3 Kit, Akoya Biosciences) for 5 min at room temperature. The samples were then counterstained with 0.5 µg/ml Hoechst 33342 in PBST for 12 min. Finally, the samples were mounted on slides in anti-fade solution (2.5% DABCO, 50% glycerol, 50% PBS) for examination.

IF staining

IF staining of fixed embryos were carried out as previously described (Khor and Ettensohn, 2017). PMCs were immunostained with monoclonal antibody (mAb) 6a9, which recognizes PMC-specific cell-surface proteins of the MSP130 family (Ettensohn and McClay, 1988; Illies et al., 2002). Embryos were fixed at the desired stage with 2% paraformaldehyde in ASW and transferred to round-bottom 96-well plates for further processing. Fixed embryos expressing GFP were incubated in blocking buffer (5% goat serum and 1% bovine serum albumin in PBS) containing a 1:2 dilution of 6a9 tissue culture supernatant and a 1:500 dilution of the anti-GFP antibody. Following several washes with PBST, they were incubated in blocking buffer containing a 1:100 dilution of Alexa Fluor 594 anti-rabbit IgG and a 1:500 dilution of DyLight 488 anti-rabbit IgG (Jackson ImmunoResearch Laboratories) for 2 h at room temperature. They were counterstained with Hoechst 33342 (0.5 µg/ml) in PBST for 12 min and mounted on slides in anti-fade solution for examination.

Acknowledgements

We are grateful to Josiah Saunders for synthesizing the RNA probes used in this study.

Competing interests

The authors declare no competing or financial interests.

Author contributions

Conceptualization: J.M.K.; Methodology: J.M.K.; Validation: J.M.K.; Formal analysis: J.M.K.; Investigation: J.M.K.; Writing - original draft: J.M.K.; Writing - review & editing: J.M.K., C.A.E.; Visualization: J.M.K.; Supervision: C.A.E.; Funding acquisition: C.A.E.

Funding

This work was supported by grants from the National Institutes of Health (R24-OD023046 to C.A.E.) and the National Science Foundation (IOS2004952 to C.A.E.). Deposited in PMC for release after 12 months.

Data availability

All relevant data can be found within the article and its supplementary information.

Peer review history

The peer review history is available online at https://journals.biologists.com/dev/lookup/doi/10.1242/dev.201373.reviewer-comments.pdf

References

Adomako-Ankomah, A. and Ettensohn, C. A. (2013). Growth factor-mediated mesodermal cell guidance and skeletogenesis during sea urchin gastrulation. *Development* **140**, 4214-4225. doi:10.1242/dev.100479

Akhtar, A. A. and Breunig, J. J. (2017). Tetracycline–inducible and reversible stable gene expression in human iPSC–derived neural progenitors and in the postnatal mouse brain. *Curr. Protoc. Stem Cell Biol.* **41**, 5A.9.1-5A.9.12. doi:10.1002/cpsc.28

Arnone, M. I., Dmochowski, I. J. and Gache, C. (2004). Using reporter genes to study cis-regulatory elements. *Methods Cell Biol.* **74**, 621-652. doi:10.1016/S0091-679X(04)74025-X

Bardhan, A., Deiters, A. and Ettensohn, C. A. (2021). Conditional gene knockdowns in sea urchins using caged morpholinos. *Dev. Biol.* **475**, 21-29. doi:10.1016/j.ydbio.2021.02.014

Brunet, A., Pagès, G. and Pouysségur, J. (1994). Constitutively active mutants of MAP kinase kinase (MEK1) induce growth factor-relaxation and oncogenicity when expressed in fibroblasts. *Oncogene* **9**, 3379-3387.

Cameron, R. A., Oliveri, P., Wyllie, J. and Davidson, E. H. (2004). cis-Regulatory activity of randomly chosen genomic fragments from the sea urchin. *Gene Expr. Patterns* **4**, 205-213. doi:10.1016/j.modgep.2003.08.007

Cheers, M. S. and Ettensohn, C. A. (2004). Rapid microinjection of fertilized eggs. *Methods Cell Biol.* **74**, 287-310. doi:10.1016/S0091-679X(04)74013-3

Cui, M., Lin, C.-Y. and Su, Y.-H. (2017). Recent advances in functional perturbation and genome editing techniques in studying sea urchin development. *Brief. Funct. Genomics* **16**, 309-318. doi:10.1093/bfgp/elx011

Czarkwiani, A., Dylus, D. V. and Oliveri, P. (2013). Expression of skeletogenic genes during arm regeneration in the brittle star Amphiura filiformis. *Gene Expr. Patterns* **13**, 464-472. doi:10.1016/j.gep.2013.09.002

Das, A. T., Tenenbaum, L. and Berkhout, B. (2016). Tet-on systems for doxycycline-inducible gene expression. *CGT* **16**, 156-167. doi:10.2174/1566523216666160524144041

Doanes, A. M., Hegland, D. D., Sethi, R., Kovesdi, I., Bruder, J. T. and Finkel, T. (1999). VEGF stimulates MAPK through a pathway that is unique for receptor tyrosine kinases. *Biochem. Biophys. Res. Commun.* **255**, 545-548. doi:10.1006/bbrc.1999.0227

Duloquin, L., Lhomond, G. and Gache, C. (2007). Localized VEGF signaling from ectoderm to mesenchyme cells controls morphogenesis of the sea urchin embryo skeleton. *Development* **134**, 2293-2302. doi:10.1242/dev.005108

Ettensohn, C. A. (1990). Cell interactions in the sea urchin embryo studied by fluorescence photoablation. *Science* **248**, 1115-1118. doi:10.1126/science.2188366

Ettensohn, C. A. and Dey, D. (2017). KirrelL, a member of the Ig-domain superfamily of adhesion proteins, is essential for fusion of primary mesenchyme cells in the sea urchin embryo. *Dev. Biol.* **421**, 258-270. doi:10.1016/j.ydbio.2016.11.006

Ettensohn, C. A. and McClay, D. R. (1988). Cell lineage conversion in the sea urchin embryo. *Dev. Biol.* **125**, 396-409. doi:10.1016/0012-1606(88)90220-5

Faedo, A., Laporta, A., Segnali, A., Galimberti, M., Besusso, D., Cesana, E., Belloli, S., Moresco, R. M., Tropiano, M., Fucà, E. et al. (2017). Differentiation of human telencephalic progenitor cells into MSNs by inducible expression of Gsx2 and Ebf1. *Proc. Natl. Acad. Sci. USA* **114**, E1234-E1242. doi:10.1073/pnas.1611473114

Fernandez-Serra, M., Consales, C., Livigni, A. and Arnone, M. I. (2004). Role of the ERK-mediated signaling pathway in mesenchyme formation and differentiation in the sea urchin embryo. *Dev. Biol.* **268**, 384-402. doi:10.1016/j.ydbio.2003.12.029

Fleming, T. J., Schrankel, C. S., Vyas, H., Rosenblatt, H. D. and Hamdoun, A. (2021). CRISPR/Cas9 mutagenesis reveals a role for ABCB1 in gut immune responses to *Vibrio diazotrophicus* in sea urchin larvae. *J. Exp. Biol.* **224**, jeb232272. doi:10.1242/jeb.232272

Gao, F. and Davidson, E. H. (2008). Transfer of a large gene regulatory apparatus to a new developmental address in echinoid evolution. *Proc. Natl Acad. Sci. USA* **105**, 6091-6096. doi:10.1073/pnas.0801201105

Gao, F., Thompson, J. R., Petsios, E., Erkenbrack, E., Moats, R. A., Bottjer, D. J. and Davidson, E. H. (2015). Juvenile skeletogenesis in anciently diverged sea urchin clades. *Dev. Biol.* **400**, 148-158. doi:10.1016/j.ydbio.2015.01.017

Guo, Y.-J., Pan, W.-W., Liu, S.-B., Shen, Z.-F., Xu, Y. and Hu, L.-L. (2020). ERK/MAPK signalling pathway and tumorigenesis (Review). *Exp. Ther. Med.* **19**, 1997-2007. doi:10.3892/etm.2020.8454

Heyland, A., Hodin, J. and Bishop, C. (2014). Manipulation of developing juvenile structures in purple sea urchins (Strongylocentrotus purpuratus) by morpholino injection into late stage larvae. *PLoS ONE* **9**, e113866. doi:10.1371/journal.pone.0113866

Illies, M., Peeler, M., Dechtiaruk, A. and Ettensohn, C. (2002). Identification and developmental expression of new biomineralization proteins in the sea urchin Strongylocentrotus purpuratus. *Dev. Genes Evol.* **212**, 419-431. doi:10.1007/s00427-002-0261-0

Kang, K., Huang, L., Li, Q., Liao, X., Dang, Q., Yang, Y., Luo, J., Zeng, Y., Li, L. and Gou, D. (2019). An improved Tet-on system in microRNA overexpression and CRISPR/Cas9-mediated gene editing. *J. Animal Sci. Biotechnol.* **10**, 43. doi:10.1186/s40104-019-0354-5

Khor, J. M. and Ettensohn, C. A. (2017). Functional divergence of paralogous transcription factors supported the evolution of biomineralization in echinoderms. *eLife* **6**, e32728. doi:10.7554/eLife.32728

Khor, J. M. and Ettensohn, C. A. (2022). Architecture and evolution of the cis-regulatory system of the echinoderm kirrelL gene. *eLife* **11**, e72834. doi:10.7554/eLife.72834

Khor, J. M., Guerrero-Santoro, J. and Ettensohn, C. A. (2019). Genome-wide identification of binding sites and gene targets of Alx1, a pivotal regulator of echinoderm skeletogenesis. *Development* **146**, dev180653. doi:10.1242/dev.180653

Khor, J. M., Guerrero-Santoro, J., Douglas, W. and Ettensohn, C. A. (2021). Global patterns of enhancer activity during sea urchin embryogenesis assessed by eRNA profiling. *Genome Res.* **31**, 1680-1692. doi:10.1101/gr.275684.121

Killian, C. E., Croker, L. and Wilt, F. H. (2010). SpSM30 gene family expression patterns in embryonic and adult biomineralized tissues of the sea urchin,

Strongylocentrotus purpuratus. *Gene Expr. Patterns* **10**, 135-139. doi:10.1016/j.gep.2010.01.002

Knapp, R. T., Wu, C.-H., Mobilia, K. C. and Joester, D. (2012). Recombinant sea urchin vascular endothelial growth factor directs single-crystal growth and branching in vitro. *J. Am. Chem. Soc.* **134**, 17908-17911. doi:10.1021/ja309024b

Kurokawa, D., Kitajima, T., Mitsunaga-Nakatsubo, K., Amemiya, S., Shimada, H. and Akasaka, K. (1999). HpEts, an ets-related transcription factor implicated in primary mesenchyme cell differentiation in the sea urchin embryo. *Mech. Dev.* **80**, 41-52. doi:10.1016/S0925-4773(98)00192-0

Lepage, T. and Gache, C. (2004). Expression of exogenous mRNAs to study gene function in the sea urchin embryo. *Methods Cell Biol.* **74**, 677-697. doi:10.1016/S0091-679X(04)74027-3

Lin, C.-Y., Oulhen, N., Wessel, G. and Su, Y.-H. (2019). CRISPR/Cas9-mediated genome editing in sea urchins. *Methods Cell Biol.* **151**, 305-321. doi:10.1016/bs.mcb.2018.10.004

Lindmark, D. G. and Müller, M. (1976). Antitrichomonad action, mutagenicity, and reduction of metronidazole and other nitroimidazoles. *Antimicrob. Agents Chemother.* **10**, 476-482. doi:10.1128/AAC.10.3.476

Luo, Y.-J. and Su, Y.-H. (2012). Opposing nodal and BMP signals regulate left–right asymmetry in the sea urchin larva. *PLoS Biol.* **10**, e1001402. doi:10.1371/journal.pbio.1001402

Margolin, J. F., Friedman, J. R., Meyer, W. K., Vissing, H., Thiesen, H. J. and Rauscher, F. J. (1994). Krüppel-associated boxes are potent transcriptional repression domains. *Proc. Natl. Acad. Sci. USA* **91**, 4509-4513. doi:10.1073/pnas.91.10.4509

Materna, S. C. (2017). Using morpholinos to probe gene networks in sea urchin. In *Morpholino Oligomers* (ed. H. M. Moulton and J. D. Moulton), pp. 87-104. New York, NY: Springer.

McIntyre, D. C., Lyons, D. C., Martik, M. and McClay, D. R. (2014). Branching out: origins of the sea urchin larval skeleton in development and evolution: Larval Skeleton Patterning. *Genesis* **52**, 173-185. doi:10.1002/dvg.22756

McMahon, A. P., Flytzanis, C. N., Hough-Evans, B. R., Katula, K. S., Britten, R. J. and Davidson, E. H. (1985). Introduction of cloned DNA into sea urchin egg cytoplasm: replication and persistence during embryogenesis. *Dev. Biol.* **108**, 420-430. doi:10.1016/0012-1606(85)90045-4

Meerbrey, K. L., Hu, G., Kessler, J. D., Roarty, K., Li, M. Z., Fang, J. E., Herschkowitz, J. I., Burrows, A. E., Ciccia, A., Sun, T. et al. (2011). The pINDUCER lentiviral toolkit for inducible RNA interference in vitro and in vivo. *Proc. Natl. Acad. Sci. USA* **108**, 3665-3670. doi:10.1073/pnas.1019736108

Morgulis, M., Gildor, T., Roopin, M., Sher, N., Malik, A., Lalzar, M., Dines, M., Ben-Tabou de-Leon, S., Khalaily, L. and Ben-Tabou de-Leon, S. (2019). Possible cooption of a VEGF-driven tubulogenesis program for biomineralization in echinoderms. *Proc. Natl. Acad. Sci. USA* **116**, 12353-12362. doi:10.1073/pnas.1902126116

Morgulis, M., Winter, M. R., Shternhell, L., Gildor, T. and Ben-Tabou de-Leon, S. (2021). VEGF signaling activates the matrix metalloproteinases, MmpL7 and MmpL5 at the sites of active skeletal growth and MmpL7 regulates skeletal elongation. *Dev. Biol.* **473**, 80-89. doi:10.1016/j.ydbio.2021.01.013

Morino, Y., Koga, H., Tachibana, K., Shoguchi, E., Kiyomoto, M. and Wada, H. (2012). Heterochronic activation of VEGF signaling and the evolution of the skeleton in echinoderm pluteus larvae: Pluteus evolution and VEGF signaling. *Evol. Dev.* **14**, 428-436. doi:10.1111/j.1525-142X.2012.00563.x

Muhammad, K. A., Nur, A. A., Nurul, H. S., Narazah, M. Y. and Siti, R. A. R. (2018). Dual-specificity phosphatase 6 (DUSP6): a review of its molecular characteristics and clinical relevance in cancer. *Cancer Biol. Med.* **15**, 14. doi:10.20892/j.issn.2095-3941.2017.0107

Nam, J., Su, Y.-H., Lee, P. Y., Robertson, A. J., Coffman, J. A. and Davidson, E. H. (2007). Cis-regulatory control of the nodal gene, initiator of the sea urchin oral ectoderm gene network. *Dev. Biol.* **306**, 860-869. doi:10.1016/j.ydbio.2007.03.033

Pedone, E., Postiglione, L., Aulicino, F., Rocca, D. L., Montes-Olivas, S., Khazim, M., di Bernardo, D., Pia Cosma, M. and Marucci, L. (2019). A tunable dual-input system for on-demand dynamic gene expression regulation. *Nat. Commun.* **10**, 4481. doi:10.1038/s41467-019-12329-9

Rafiq, K., Cheers, M. S. and Ettensohn, C. A. (2012). The genomic regulatory control of skeletal morphogenesis in the sea urchin. *Development* **139**, 579-590. doi:10.1242/dev.073049

Rafiq, K., Shashikant, T., McManus, C. J. and Ettensohn, C. A. (2014). Genome-wide analysis of the skeletogenic gene regulatory network of sea urchins. *Development* **141**, 950-961. doi:10.1242/dev.105585

Röttinger, E., Besnardeau, L. and Lepage, T. (2004). A Raf/MEK/ERK signaling pathway is required for development of the sea urchin embryo micromere lineage through phosphorylation of the transcription factor Ets. *Development* **131**, 1075-1087. doi:10.1242/dev.01000

Saunders, L. R. and McClay, D. R. (2014). Sub-circuits of a gene regulatory network control a developmental epithelial-mesenchymal transition. *Development* **141**, 1503-1513. doi:10.1242/dev.101436

Sharma, T. and Ettensohn, C. A. (2010). Activation of the skeletogenic gene regulatory network in the early sea urchin embryo. *Development* **137**, 1149-1157. doi:10.1242/dev.048652

Sharrock, A. V., Mulligan, T. S., Hall, K. R., Williams, E. M., White, D. T., Zhang, L., Emmerich, K., Matthews, F., Nimmagadda, S., Washington, S. et al. (2022). NTR 2.0: a rationally engineered prodrug-converting enzyme with substantially enhanced efficacy for targeted cell ablation. *Nat. Methods* **19**, 205-215. doi:10.1038/s41592-021-01364-4

Shashikant, T., Khor, J. M. and Ettensohn, C. A. (2018). From genome to anatomy: The architecture and evolution of the skeletogenic gene regulatory network of sea urchins and other echinoderms. *Genesis* **56**, e23253. doi:10.1002/dvg.23253

Shin, K.-J., Wall, E. A., Zavzavadjian, J. R., Santat, L. A., Liu, J., Hwang, J.-I., Rebres, R., Roach, T., Seaman, W., Simon, M. I. et al. (2006). A single lentiviral vector platform for microRNA-based conditional RNA interference and coordinated transgene expression. *Proc. Natl. Acad. Sci. USA* **103**, 13759-13764. doi:10.1073/pnas.0606179103

Sun, Z. and Ettensohn, C. A. (2014). Signal-dependent regulation of the sea urchin skeletogenic gene regulatory network. *Gene Expr. Patterns* **16**, 93-103. doi:10.1016/j.gep.2014.10.002

Tarsis, K., Gildor, T., Morgulis, M. and Ben-Tabou de-Leon, S. (2022). Distinct regulatory states control the elongation of individual skeletal rods in the sea urchin embryo. *Dev. Dyn.* **251**, 1322-1339. doi:10.1002/dvdy.474

Wessel, G. M., Kiyomoto, M., Shen, T.-L. and Yajima, M. (2020). Genetic manipulation of the pigment pathway in a sea urchin reveals distinct lineage commitment prior to metamorphosis in the bilateral to radial body plan transition. *Sci. Rep.* **10**, 1973. doi:10.1038/s41598-020-58584-5

Yamazaki, A., Yamakawa, S., Morino, Y., Sasakura, Y. and Wada, H. (2021). Gene regulation of adult skeletogenesis in starfish and modifications during gene network co-option. *Sci. Rep.* **11**, 20111. doi:10.1038/s41598-021-99521-4

Yuh, C. H. and Davidson, E. H. (1996). Modular cis-regulatory organization of Endo16, a gut-specific gene of the sea urchin embryo. *Development* **122**, 1069-1082. doi:10.1242/dev.122.4.1069